Numerical Simulation of Interfacial Debonding in Particulate Composites Considering Material Inhomogeneities

Panayiotis Kakavas

Technological Educational Institute of Patras, Greece

*Nick Anifantis**

Mechanical and Aeronautics Engineering Department, University of Patras, Greece

Summary: A comparative study in the framework of large deformations has been conducted to get insight into micro mechanical response of particulate polymeric composites. The propound model enables finite element predictions of displacement response and resulting debonding of a three-phase material subjected to incremental loading conditions. Predictions employ a unit cell of certain shape under specified loading and constraints. The proposed model involves nonlinear material properties and incorporates a strong or weak non-homogeneous interphase region. The interphase toughness is expressed in terms of the adhesion efficiency between the filler and the matrix, though contact conditions are preserved utilizing special contact elements. Interfacial nonlinear spring joint elements regulate debonding initialization, in relation to the imposed failure criterion. Numerical results are presented and discussed for axial tensile and compressive loadings for a variety of values of the imposed parameters.

Introduction

As the demands on strength and durability of today's engineering materials increase, the advantages of combining the properties of two or more materials into a single member have become apparent. However, the combination of material properties can contribute to failure of structures, although it is of particular interest the integrity of junction between the constituents. Considering idealized conditions, these materials often consist of stiff spherical fillers embedded in a

 CCC 1022-1360/00/$ 17.50+.50/0

soft matrix. In order to rationalize the design of reinforced materials it is of primary importance to have a detailed knowledge of stress concentration induced by the applied load. Debonding is the result of overloading in conjunction with nonlinear behavior of the material expressed in terms of damage criteria, like plasticity, fracture, etc. Several experimental, analytical and numerical methods exist in order to investigate the interfacial conditions. In this context, to describe the progressive debonding behavior various researchers utilize finite element method incorporating fracture criteria that are combined with material damage models. Filler bonding results from diffusion or chemical reactions and possibly the filler clamping from residual stresses. In most composites interfaces extend to an interphasial thin layer consisted of one or several materials deposited on the filler like a coating. Experiments and numerical models have demonstrated that a strong interphase is beneficial to the strength, toughness, lifetime and creep resistance.[1] However, a major concern is that the mechanical performance of composites may deteriorate upon being exposed to extreme environmental conditions. The interphase region is susceptible to such attack and thus attention on this must be focused. The concept of strong interphase has been established on polymeric coated filler composites.[2] Filler debonding results in from the deflection of the cracks that initiate in the matrix. The mechanism of debonding in strong interphase composites is different than the one occurring in weak composites. Both of these phenomena are not clear and are unresolved.

The calculation of stress concentration around a particle embedded within a matrix material has been the concern for many years. The mechanisms for craze and shear band formation were previously investigated for small glass beads embedded in polymeric matrices, such as, polystyrene and polycarbonate subjected to uniaxial tension.[3] For perfectly adhering glass bead in polystyrene matrix the crazes are formed near the poles of the reinforcement. At these regions the stress analyses has shown that maximum dilatation and principal stress exists. For perfectly adhering glass bead in a polycarbonate matrix the shear bands form near the surface of the particle at 45^0 from the poles. These are the regions of maximum principal shear stress and maximum distortion strain energy density. In

the case, of poor adhesion between the two phases, both craze and shear band formation, along the interface between particle and matrix are preceded by dewetting. At dewetting a curvilinear crack is formed starting at the pole and propagating in the direction of the equator until 60^0 where a craze or shear band originates at the tip of the interfacial crack. A theoretical analysis was given for detachment of an elastomer from a rigid spherical inclusion by a tensile stress applied to the specimen.[4] The catastrophic debonding is predicted to occur at a critical applied stress when the initial debonds is small. Detachment is assumed to start at an already debonded region and take place by grown of this debonded region when the elastic strain energy thereby released in the matrix is greater than the energy required for further debonded. This statement is a direct application of the Griffith's criterion. The amount of strain energy lost from the system as a result of debonding can be evaluated from the difference between the strain energy levels before and after debonding has taken place. The establishment of a unit cell appropriate for debonding simulations in particulates reinforced with spherical fillers is an alternative numerical procedure.[5] The stress-strain state of the cell has been calculated in the framework of the large deformation approach within a wide range of filler volume concentrations. The choice of the form and loading conditions for structural elements is the most important stage in searching for an adequate simulation of particulate composites behavior. The Griffith's approach was used to describe the initiation and propagation of debonds where the postulates of the existence of small precursor debonds and the invariance of debonds energy during crack growth was adopted. It was shown, that the most probable point of debonding is located at the region of the inclusion's pole where maximum strain and hydrostatic extensions are concentrated. The energy required for further matrix detachment has been defined as the rate of change of the energy increment of our system needed to increase the crack area. This energy is a characteristic of the system matrix-inclusion regarded as the cohesive or adhesive tear energy. The only energy source for debonding is the current strain energy accumulated in the matrix. The tear strength of the matrix may be considered as a magnitude that provides the ultimate bond strength. The threshold tear strength of

the matrix correlates with the modulus of elasticity of the material.[4] The elastic properties of a three-phase composite made up of spherical particles coated with a mesophase and dispersed in a continuum matrix were computed through a periodic microfield approach.[6] The interfacial debonding processes in Al/Sic metal matrix composites using three dimensional finite element computations on representative cells has been reported elsewhere.[7] The reinforcements are considered as elastic, while an elastoplastic law describes the behavior of the matrix. The concept of interphase was used for modeling the problem of fiber and/or particulate composites.[8-10]

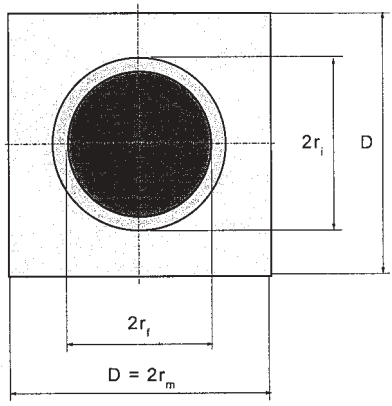

Figure 1. Geometry of the unit cell model.

In an attempt to better understanding the influence of the interphase modulus on the stress transfer characteristics and the debonding process of an axially loaded single spherical particle embedded in a matrix, a computational procedure was developed in the present work. This improved micromechanics analysis investigates the effect of imperfect adhesion and interphase weakness on fracture failure in particulate composite systems. A generalized representative volume element with axially symmetric geometry was chosen, consisting of a spherical filler surrounded by other phases. The matrix and the filler have uniform

properties while the interphase have the Young's modulus varying in the radial direction. In order to investigate the influence of the involved parameters to the failure mechanism, a computational analysis has been performed, implementing a regenerative finite element approach, which permits presence of material and strength imperfections. Numerical results illustrate and discuss the evolution of debonding process with load distribution and direction, strength and interfacial adhesion, material inhomogeneities and material damage model.

Non-Homogeneous Interphase

The establishment of a unit cell as unit material configuration appropriate for numerical simulations, based on physical concepts and without enlisting macroscopic notions, may be regarded as a vital problem in today's materials science. In this context, the unit cell considered here is an extension of that proposed in literature.[11] In this cylindrical cell, the spherical filler is embedded on the center of the epoxy matrix. The height of the cylinder is equal to its diameter, i.e., $D = 2r_m$. The radii of the spherical filler and the cylindrical matrix are r_f, r_m, respectively. Around the filler extends an interphasial layer having width $\Delta r = r_i - r_f$ (Figure1). Material properties of the interphase region differ from respective ones of filler and matrix. Physical and chemical reasons require for the interphase properties to comply with those of adjacent phases, enforcing thus strong gradients within this region. Utilizing bulk material properties of filler and matrix in modeling issues of interphase properties[10], the exponential variation in properties of interphase was chosen in the present study for its simplicity and completeness. In order to formulate a generalized model, the filler is assumed to be linearly elastic and the matrix elasto-plastic. The indices f, i and m define material phases of the unit cell.

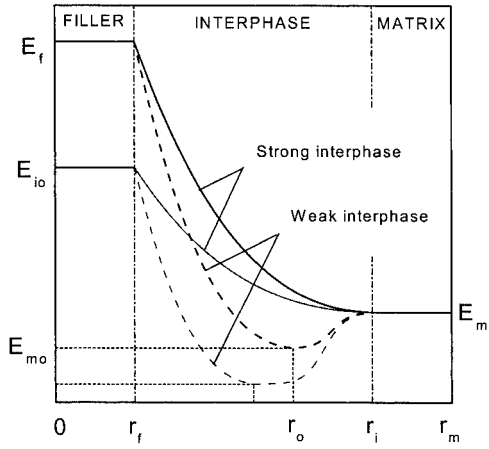

Figure 2. Variation of the modulus of elasticity within the unit cell.

Considering the modulus of elasticity as the dominant material property in stress analysis problems and ignoring Poisson's ratio effects, the variation of the modulus of elasticity within the interphase is shown in Figure 2. An equivalent way to model the degree of debonding between the fiber and matrix lies on the formulation of a simultaneously compliant and imperfect interphase that has lower stiffness than that of the filler and preserves continuity of tractions and displacement at the interphase-matrix interface. This feature of imperfect adhesion is regulated through the ratio $\alpha = E_{io}/E_f$, where E_{io} is the reduced elastic modulus of interphase on $r = r_f$. The upper limit value $\alpha = 1$ describes a compliant three-phase model without jumps on elastic modulus at $r = r_f$, although, the lower limit $\alpha = E_m/E_f$, involves a two-phase model (Figure 2). In this case, the adhesion and subsequently the interphase stiffness decrease to minimum levels, but no material separation or similar type failures occur. When $E_m/E_f \le \alpha \le 1$, intermediate three-phase models are established. This general formulation describes imperfect adhesion as an extension of the perfect one, by assigning proper values to the adhesion factor α.

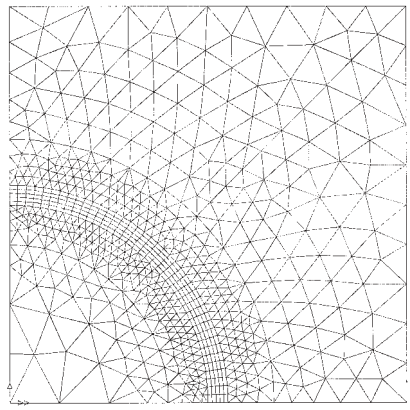

Figure 3. Finite element grid.

The present model involves also a weak interphase by including the presence of impurities, damages or yielding. To a certain extend, this type of weakness is suggested by the cure chemistry of epoxy resin. This type of failure is equivalently simulated by a loss of the interphase stiffness, which may be lower than that of the matrix. Factor $\beta = E_{mo}/E_m$, which varies in the range $0 \le \beta \le 1$, express the interphase weakness feature of the model, where E_{mo} is the minimum value of elastic modulus within interphase, occuring on $r = r_o$. Interphase weakness may be affected on third factors like Poisson's ratio variations. Since both the inhomogeneity and stress concentration due to the Poisson ratio are much smaller that those due to the elastic modulus, Poisson effect is neglected here without loss of generality. This general model involves a compliant interphase on the side of the matrix, imperfect on the side of the fiber, and softer than the fiber and matrix in the between. While the first of these features lies on manufacturing reasons, the other two simulate imperfect adhesion and damaged interphase situations. They are independent of each other, may exist or not, and their magnitude is controlled through adhesion and loss stiffness factors, respectively.

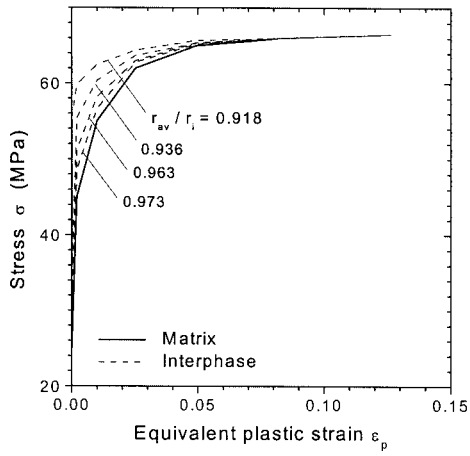

Figure 4. Nonlinear stress-stain behavior of unit cell materials.

Depending on the strength of the intrphase, the modulus of elasticity within the interphase is then assumed to vary, as

$$E_i(r) = E_m\,[1 + (\alpha q - 1)\,R_s(r)] \tag{1}$$

$$E_i(r) = E_m \begin{cases} \beta[1 + (\alpha q - 1)\,R_w(r)], \text{ when } r_f \le r \le r_o \\ 1 + (\beta - 1)\,Q(r), \quad \text{when } r_o \le r \le r_i \end{cases} \tag{2}$$

where Equation (1) defines a strong and Equation (2) a weak interphase, respectively. In above equations, the ratio $q = E_f/E_m$, express the overall composite inhomogenuity, and the functions,

$$R_s(r) = \frac{1 - (r/r_i)\exp(1 - r/r_i)}{1 - (r_f/r_i)\exp(1 - r_f/r_i)} \tag{3}$$

$$R_w(r) = \frac{1-(r/r_o)\exp(1-r/r_o)}{1-(r_f/r_o)\exp(1-r_f/r_o)} \tag{4}$$

$$Q(r) = \frac{1}{1+\exp((r-r_c)/c)}, \tag{5}$$

the exponential variation in the transverse direction. The parameter $r_c = (r_o + r_i)/2$, determines the slope of stiffness, c being a constant. Although this model can easily expanded to involve other types of imperfections, in the present paper general spatial inhomogeneities within the interphase, different than those reported above are ignored. Many different interphases can be modeled by varying the parameters α, β, and the type of weakness.

Table 1. Material properties.

Material	E (GPa)	ν	Yield stress (MPa)
Glass filler	70.00	0.220	-
Epoxy matrix	3.50	0.350	25

Table 2. Experimental stress-strain response of epoxy matrix.

Engineering strain (%)	Stress (MPa)
1	25
2	45
3	55
4	62
5	65
6	66
7	66.5

Computational Procedures

While analytical models usually are of simple geometry and boundary conditions, the finite element method employs the same exact mathematical procedure in problem solving and yet possesses the flexibility for complex geometry, inhomogeneous material and boundary conditions modeling. In this study, in order to elucidate the role of unit cell morphology, interphase weakness and imperfect adhesion mechanisms, the deformation, stress response and failure of filler-reinforced composites was numerically investigated. The inherent nonlinearities render the problem unresolved by analytical procedures, leading to numerical approximations. Among these, the finite element method is adopted for its simplicity, generality and ability to treat inhomogeneous nonlinear failure problems effectively. A computational model has been developed that enables stress and failure analysis of any material inhomogeneity by defining the model features by means of appropriate global variables. To reduce the size and the complexity of the procedure, the analysis is performed on a representative unit cell consisted from a spherical filler embedded in a polymeric matrix. Between these phases, extends an inhomogeneous interphase region. A regenerative finite element procedure was developed, which allows solution of any particular composite construction, accounting variations in domain, materials, toughness, weak interphase and imperfect adhesion. Then global design variables include geometric parameters, constituent material properties, and interphase weakness coefficients. Accounting the nodal coordinates for each element lying within the interphase, the elastic moduli are then evaluated and assigned by means of Equations (1) and (2). A computer algorithm was developed in order to evaluate the elastic moduli within the interphase, for the given particular values of the global variables. Within the interphase, material properties then vary in a piecewise manner approaching the exponential variations.

The specificity of the cylindrical unit cell provides a better fit between the modeled and realistic behavior of particulate composites at high filler volume fraction. The radius of the inclusion is a measure of the filler volume fraction. When this radius increases until it touches the lateral surface of the cell, the

maximum filler volume fraction is reached. This value is close to that characterizing the ultimate packing of random structures composed of the uniformly sized spheres.[11] The solution of the nonlinear debonding problem has been solved utilizing finite element procedures. Although numerical results are depicted for a particular case, the modeling is quite general and may produce results for any value for filler volume fraction.

(a) (b)

Figure 5. Contours of axial displacement component of the deformed unit cell on, (a) debonding initiation, and (b) fracture propagation.

The finite element mesh adopted for numerical predictions is shown in Figure 3. This model consists of 960 triangular, 200 rectangular and 40 interface, axially symmetric elements, and totally of 15596 nodes. The interphase subdomain has been modeled adopting five layers of axially symmetric rectangular elements. The interface elements are used at filler-interphase interface potential debonding surface to model interphasial failure, and crack initiation and propagation, in an incremental nonlinear analysis. These four-node axially symmetric elements have no geometric properties and connect conjugate nodes of filler surface to corresponding ones of interphase internal surface with nonlinear springs. They have initially zero thickness, but when some relative displacement between the conjugate node pairs and some initiation stress level are simultaneously enabled under loading increase conditions, then failure starts permitting softening of springs followed by large opening displacements. The material toughness is a

measure of fracture energy required to debonding initiation process. Depending on the failure process orientation, they describe opening, shearing or complex mode fractures.

(a) (b)

Figure 6. Contours of radial stress over the deformed unit cell configuration, (a) on the debonding initiation, and (b) on fracture propagation.

Table 1 describes the material properties of the constituent materials. The glass filler is considered as perfectly elastic and the epoxy matrix as nonlinear elastic with experimentally measured stress-strain behavior as that shown in Table 2. To be the material properties of the interphase compliant to those of filler and matrix, it has been assumed that the interphase presents nonlinear elastic behavior with progressive stiffening as the filler is approached. Thus, the stress-strain response of the interphase is a function of radial abscissas. In the case of a strong interphase with $\alpha = 0.85$, Figure 4 illustrates the average values of stress-strain characteristics of interphasial layers. Assuming nonlinear material hardening convention, the equivalent plastic strain ε_{pi} was evaluated with the help of Equations (1-2) and Table 1, by the relation

$$\varepsilon_{pi}=\varepsilon_{pi-1}+\varepsilon_i-\sigma_i/E \qquad (6)$$

where ε_i, σ_i are the strain and stress pairs shown in Table 2, respectively, i being

the sequence order. The slopes s_i of the curves in Figure 4, have been accordingly evaluated as follows

$$s_i = E_i/(1 - E_i/E) \tag{7}$$

In above Equations, $E_i = (\sigma_i - \sigma_{i-1})/(\varepsilon_i - \varepsilon_{i-1})$ is the linearized modulus of elasticity, $E = \sigma_y/\varepsilon_y$ is the conventional modulus of elasticity, $\varepsilon_y = \varepsilon_1$ and $\sigma_y = \sigma_1$ being the yield strain and stress, respectively. Thus, particular nonlinear material models of the interphase may be constructed in terms of the global variables of the problem.

(a) (b)

Figure 7. Contours of axial stress over the deformed unit cell configuration, (a) on the debonding initiation, and (b) on fracture propagation.

The consistensy of the unit cell with the macroscopic behavior of the composite, requires application of a constraint on the lateral surface to keep its shape under deformation. On the top surface of the model, extentional or compressive loading in the form of prescribed vertical displacement it is applied, and on the other sides, usual symmetry conditions are valid. The nonlinear behavior is governed by an elastoplastic constitutive law, which is formulated with a Mohr-Coulomb criterion. Since it is no longer possible to directly obtain a stress distribution, which equilibrates a given set of external loading, an incremental solution

procedure has been adopted. At each increment, a linear prediction of the nonlinear response is made, and subsequent iterative corrections are performed in order to restore equilibrium by the elimination of the residual or out of balance forces.

(a) (b)

Figure 8. Contours of shear stress over the deformed unit cell configuration, (a) on the debonding initiation, and (b) on fracture propagation.

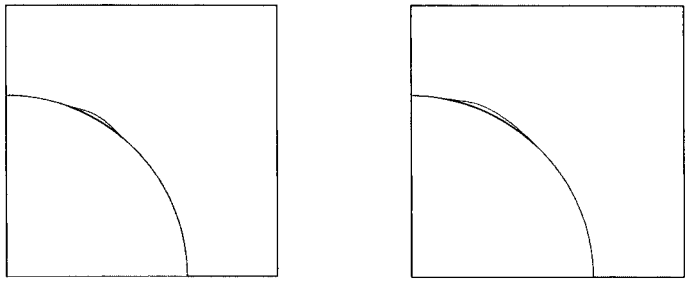

(a) (b)

Figure 9. Sketches showing debonding process evolution under extensional loading on (a) debonding initiation, and (b) fracture propagation stages.

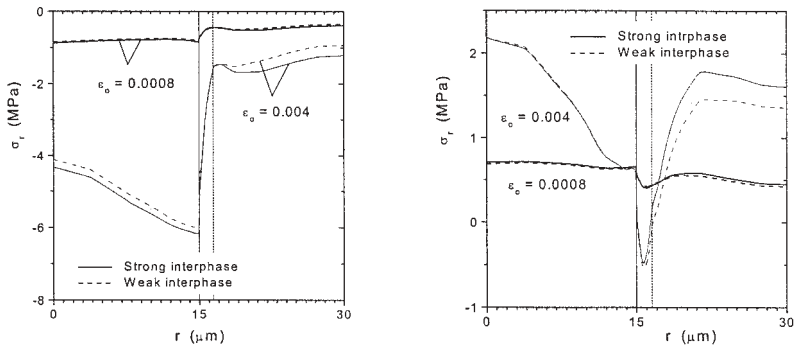

(a) (b)

Figure 10. Variation of radial stress in the direction of the equinoctial plane of the unit cell when is subjected, (a) to tension, and (b) to compression.

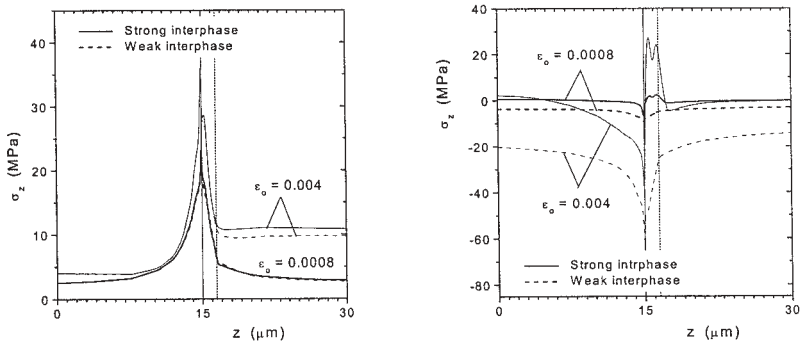

(a) (b)

Figure 11. Variation of axial stress in the direction of axis of symmetry of the unit cell when is subjected, (a) to tension, and (b) to compression.

Numerical Results

In order to investigate the effect of a non-homogeneous interphase on debonding failure process developed within particulates, the computational simulation outlined above has been applied. The particulates used in the present investigation consist of an epoxy matrix reinforced with spherical glass particles. Omitting the

long and tedious details, the problem is reduced to several finite element solutions, which yield the desired failure prediction. Varying the global variables of the problem, numerical results were obtained concerning the stress and deformation states, and failure process of particulate composites. To reduce the computational effort, it was assumed that the radius of the filler is $r_f = 15\,\mu m$, the radius of the matrix $r_m = 30\,\mu m$, and the normalized thickness of the interphase $\Delta r_i/r_f = 0.1$. Without loss of generality, numerical results illustrated in the following regard two particular cases. Both incorporate imperfect adhesion conditions between filler and matrix, and presence of strong or weak interphase. Thus, the mechanical properties of the unit cell are such that the composite characterizing parameters have the specific values $q = 28$, $\alpha = 0.85$, and $\beta = 0.5$, for the strong and weak interphase cases, respectively. For the properties of the interface elements, the fracture energy was taken 150 Joule, the initiation stress 65 MPa and the maximum relative displacement $0.001\,\mu m$.[5]

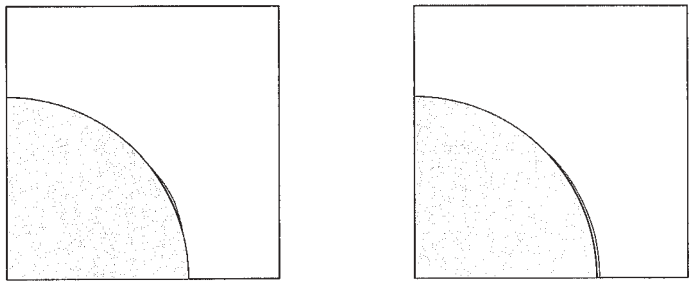

(a) (b)

Figure 12. Sketches showing debonding process evolution under compressional loading on (a) debonding initiation, and (b) fracture propagation stages.

Initially the convergence of the procedure was investigated, considering various mesh refinements, increment magnitudes and relative interfacial displacements. Results shown in the following refer to optimized parameters of the procedure, for which convergence is attained. Based on very dense mesh refinement scheme,

propound model does not invlove treatment of field singularities with crack elements, which complicate significantly the numerical procedures. Thus, stress singularities can be only seen as "moving" stress concentrations ahead debonding tips. Considering extensional loading conditions, the two cases are illustrated in the following, regard the applied strains on the top surface of the unit cell $\varepsilon_0 = 0.0005$ and $\varepsilon_0 = 0.004$, which correspond to debonding initiation and some fracture extension, respectively. To be the results more clear, an exaggeration factor of 20 was applied to the deformed shapes. For comparison reasons, the outline of undeformed original shape of the unit cell is drawn also by solid lines. A color key scale of 20 colors was adopted, red and blue being the maximum and minimum values, respectively, while other colors indicate intermediate values. Figure 5 depicts the contours of the axial displacement component. The location of the debonding initiation lies about 30° lower than the pole of the particle and is identical to that experienced experimentally. From this point a crack initiates and propagates simultaneously to the pole and equator positions. When the region of the pole debonds, a depth open crack is formed. The deformations of the particle are very small while within the interphase step deformation gradients develop. Figures 6.a and 6.b illustrate the contours of radial stress at the same loading increments, which correspond to debond initiation and at some crack depth, respectively. It is obvious the stress concentration in the region of interphase and especially in the locus of debond initiation. The fracture propagation is shown to release stresses and fracture surfaces become traction free. Figures 7 and 8 illustrate the contours of axial and shear stresses, respectively, on the same loading increments. A detailed examination of these Figures explains the locus position of initial debonding. Where some relative displacement occurs and simultaneously some high stress is developed, there debonding starts. The rate of crack propagation in both tips depends on both the stress concentration and the relative deformations produced on increase of loading (see Figure 9).

When the unit cell is subjected to extensional or compression loading, Figures 9 and 10 depict a comparison of between radial and axial stress distributions, respectively. Radial stress distribution is close to the equator ($z \approx 0$), although

axial stress distribution lies on the axis of symmetry ($r \approx 0$). Numerical results are plotted for two absolute values of the applied strain on the top surface of the cell, i.e., $\varepsilon_o = 0.0008$ and $\varepsilon_o = 0.004$, which correspond to debonding initiation and to the development of some fracture, respectively. In all cases shown, imperfect adhesion is valid with $\alpha = 0.85$. This value has been chosen close to perfect case ($\alpha = 1.0$), in order to study the sensitivity of the debonding process to small changes in the involved parameters. The weak interphase regards a situation where $\beta = 0.5$. Interphase weakness a little affects the stress distribution. In the axial direction, at some time instants high stress concentration occurs that does not yield debonding because the relative displacement is small enough. Generally speaking, the extensional loading yields more intense stress fields than the corresponding compressive. Under compressive loading, the debonding process is different than that observed under tensional loading (see Figure 12). In the former case the filler behaves like a solid body, the debonding starts on the side of the equator and very small crack opening deformations occur. When tensile or compressive loading is applied, Sketches 9, 12 and Figures 10, 11 explain somewhat the difference in the debonding mechanism as affected by the particular shape of unit cell and imposed lateral constrains. At the tips of the debonding surface, which is axially an interfacial crack, high stress intensification occurs featuring the principles of fracture mechanics.

Conclusion

A generalized computational model has been developed for the prediction of the debonding characteristics of particulate composites incorporating a heterogeneous interphase region. This model enables simulations of both imperfect adhesion and interphasial weakness by proper formulation of the interphase properties. Then, numerical studies were conducted to demonstrate how the interphase strength and the adhesion efficiency affect the local deformation and stress states and so forth the fracture mechanisms. The loci of high stress concentration and step stress

gradients are investigated and inter-related to failure initiation and propagation process. Although the interphase plays a crucial role in the development of load transfer mechanisms, the presence of material imperfections within this region intensifies stress gradients and causes stress relaxation of the material structure. Present model is general and may be used for further analysis and hence provide a basis for further understanding of the toughening mechanism for fiber bridging.

[1] B. T. Lauke, T. Schuller, W. Beckert, *Computational Materials Science* **2000**, 18, 362.
[2] F. J. Rebillat, J. Lamon, A. Guette, *Acta Materiallia* **2000**, 48, 4609.
[3] M. E. J. Dekkers, D. Heikens, *Journal of Materials Science* **1985**, 20, 3865.
[4] A. Gent A, *Journal of Material Sciences* **1980**, 15, 2884.
[5] V. V. Moshev, L. L. Kozhevnikova, *Inter. Journal of Solids and Structures* **2000**, 37, 1079.
[6] J. M. Llorca, M. Elices, Y. Termonia, *Acta Materiallia* **2000**, 48, 4589.
[7] H. Haddadi, C. Teodosiu, *Computational Materials Science* **1999**, 16, 315.
[8] J.L. Chaboche, R. Girard, A. Schaff, *Computational Mechanics* **1997**, 20, 3.
[9] J.Y Li, *International Journal of Solis and Structures* **2000**, 37, 5579.
[10] C. C. Kiritsi, N. K. Anifantis, *Computational Materials Science* **2001**, 20, 86.
[11] J.D. Bernal, G. Mason, *Nature* **1960**, 4754.